Exergoeconomic Analysis of a Direct Expansion Solar Assisted Heat Pump for Humid and Tropical Climates

Francis Gorozabel-Chata[1*], Tania Carbonell-Morales[2], Roxana Panchana-Cedeño[3]

[1]*Mechanical Engineering Department, Technical University of Manabí, Portoviejo, Ecuador; E-mail: Francis.gorozabel@utm.edu.ec*

[2]*Universidad Tecnológica de la Habana, CUJAE, La Habana, Cuba*

[3]*Economic Department, Technical University of Manabí, Portoviejo, Ecuador*

Abstracts: A direct expansion solar assisted heat pump (DX-SAHP) is a heating water technology that convey a conventional solar heating system with a heat pump. This technology with great potential should overcome economics aspects to be available commercially soon. An exergoeconomic analysis of a DX-SAHP has been performed for three collector configurations and three compressor displacement capacity under the meteorological condition of Portoviejo city in Ecuador, a location with a tropical and humid climate. The present work is aimed to study the relationship between exergoeconomic data under various operations conditions. In addition, the exergy destruction, exergetic efficiency, cost rate per exergy unit product and fuel, cost rate associated to exergy destruction, exergoeconomic factor for each component of a DX-SAHP are evaluated. The exergoeconomic factor is found lowest for the solar collector for all the configurations, with estimated values of 5 to 21%. The component that needs more improvement for a tropical and humid climate is the solar collector based on exergoeconomic factor. On the basis of the present study, it can be concluded that a solar collector area of 1,5 m2 and a rotational displacement capacity of 1350 rpm performs better in all respects.

Keywords: Exergoeconomic Analysis, Exergy Analysis, Solar Energy, Heat Pump, Economic Analysis.

1. INTRODUCTION

A DX-SAHP system is a technology with a great potential to become a viable alternative for industries that use fossil fuels for hot water production, food crop drying and space heating [1-4]. In the last five years some technological progress has been made that allows it to be commercialized [5], however, to penetrate the current market [6] this technology should improve exergetic efficiency while simultaneously reducing equipment cost, to deal with this problem researchers must understand the real mechanism according to which thermodynamics inefficiencies and costs are formed [7].

Exergy-based methods is a suitable technique to optimize an energy conversion system [8], exergy is defined as the maximum theoretical useful work obtainable from an energy conversion system as this is brought into thermodynamic equilibrium with the thermodynamic environment while interacting only with this environment [4]. An exergy-based thermodynamic analysis identifies the location, the magnitude, and the causes of thermodynamic inefficiencies, these thermodynamic inefficiencies which are exergy destruction (due to irreversibility within the system) and exergy loss (exergy transferred to the environment) [9].

An exergoeconomic analysis is a unique combination of cost and exergy analysis conducted at the component level, which provides the designer or researcher of a power conversion system with crucial information for the design of an efficient system with low costs [10].

Chaturvedi et al. [11] perform an economic analysis of a direct expansion solar assisted heat pump using the life cycle cost (LCC) method, the analysis reveals that the minimum value of the system life cycle cost is achieved at optimal values of the solar collector area as well as the compressor displacement capacity. Rabelo et al. [12] showed that there is an economically optimum size of collector area for the DX SAHP, which it is the same for different environmental conditions.

Hepbasli et al. [13] used the specific exergy cost (SPECO) method to calculate exergy-related parameters and display cost flows for all streams and components in of a mobile air conditioning system. Singh et al.[14] used a batch-type solar-assisted heat pump dryer (SAHPD) for closed system drying of banana chips, It is observed that the most important components that needed to improve based on exergoeconomic factor are expansion device and evaporator.

Several works have been publishing about exergoeconomic analysis of energetics system [13-18]. The goal of the present work is to analyze the exergoeconomic factor of a direct expansion solar assisted heat pump for three collector area configurations and three compressor rotational displacement for tropical and humid climate. The above aspect of a DX-SAHP is the novel feature of this study, and to the best of the author´s knowledge, it has not been described in the present literature.

2. MATERIAL AND METHODS

2.1 Description of the DX-SAHP System

The aim of this experimental procedure is to characterized from an exergoeconomic point of view the behavior of this technology, exergoeconomic variables such as exergy destruction, exergy efficiency, the cost rate of exergy destruction rate, total cost rate and exergoeconomic factor for each component are discussed. The experiments were carried out under the meteorological conditions of Portoviejo (latitude of 0°N, longitude of 75.49 E), Ecuador a city with a climate with tropical and humid climate, from August to October 2019 at the Mechanical Engineering Department of the Technical University of Manabí.

2.2 Experimental Set Up

A DX-SAHP experimental set up has four components; the tank-type condensate; a bare solar collector; a compression unit; and an electronic expansion valve. The schematic diagram of a DX-SAHP used to conduct the present experiment is depicted in Figure 1. A photograph of the experimental set up is shown in Figure 2. Three serpentines solar collectors, which act as an evaporator, were connected in series. A copper tube of 9.52 mm diameter was soldered at the back of 0,57 mm thick copper fin absorber plate. Adequate insulations were provided at the back of the collector but no glass cover used on the top surface. There is a bypass line from the exit of the first collector/evaporator to the exit of the second and the third, which remains closed or open depending on the solar irradiation and the speed of the compressor. The ambient air also acts as a heat source depending on the operator temperature of the evaporator/collector.

The condenser was made up of a coil copper tube of 9.52 mm of diameter with length 60 m, which was immersed in the domestic hot water tank (with water volume 250 L, and Polyurethane insulation thickness 50 mm), and a filter drier was installed downstream the condenser. A R-134A-based hermetically sealed reciprocating compressor is used for the system. Which is directly coupled to a three-phase induction motor. A frequency inverter is used to control the speed of the motor. An electronic expansion valve controls the superheat and the mass flow of the refrigerant.

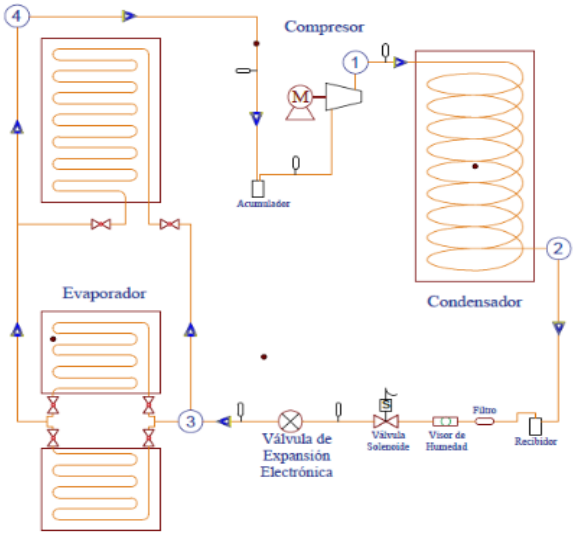

Figure 1. Control points in a DX-SAHP

Figure 2. Frontal view of a direct expansion solar assisted heat pump

2.3. Instrumentation

Four calibrated temperature sensors (Pt 100) with an accuracy of ± 0.5 K were in the refrigerant line at compressor suction and discharge, condenser outlet and electronic expansion valve outlet (to measure the temperature at salient points in the DX-SAHP system). The ambient temperature was measured with the help of a thermometer of ± 0.5 K accuracy. Two pressure transducers with an accuracy ± 1 % were fixed at compressor suction and discharge for the measuring the corresponding pressures. To check the pressure at salient points, four bourdon pressure gauge with ± 2% accuracy were installed. All the temperature sensors and pressure transducer were connected to the computer through a data acquisition system. A Pyranometer with an accuracy of ± 5 W m^{-2} was placed near the solar collector to measure the instantaneous solar intensity.

2.4 Experimental Procedure

The heat pump was initially flushed with nitrogen gas to remove the impurities and moisture inside the system and charged with R-134A. During experimentation, the temperature of the refrigerant at different points in the refrigeration system, and the pressure at four salient points were recorded automatically in the computer. All these

readings were fetched by software installed in the computer periodically at every 60 s. The solar radiation falling on the solar collector (evaporator), the temperature of water at the inlet and outlet of condenser were manually measured. The experiments were carried out only during sunshine hours. The experimental data thus obtained where use for analyzing the exergoeconomic factor of a DX-SAHP

2.5 Uncertainty Analysis

The uncertainty analysis of the various calculated parameters is estimated according to Holman [19]. In the present study pressures, temperatures, solar radiation, were measured with instruments as mentioned in the previous section. The uncertainty arising in calculating a result due to several independent variables given by Eq. (1).

$$W_r = \left[\left(\frac{\partial R}{\partial x_1} w_1\right)^2 + \left(\frac{\partial R}{\partial x_2} w_2\right)^2 + \cdots + \left(\frac{\partial R}{\partial x_3} w_3\right)^2\right]^{1/2} \quad \textbf{(1)}$$

Here, R is a given function, w_r the total uncertainty, $x_1, x_2, \ldots, x_n$ the independent variables and $w_1, w_2, \ldots w_n$ the uncertainty in the independent variables. The uncertainties for the calculated parameters such as the exergoeconomic factor of compressor, condenser, electronic expansion valve, and solar collector are calculated as 7.6, 7.3, 6.4 and 8.1 % respectively.

2.6 Methodology

An exergoeconomic analysis procedure consist in four steps [16]. As a first step, the mass, and energy data should be fulfilled by an experimental set up [20]. Second, by using the exergy data of each stream, the exergy of fuel and product are formulated for each system component and the overall system [4]; then, the exergy destruction, exergy destruction ratio (Eq. (4)), and exergetic efficiency (Eq. (2)) are calculated [21-23] and used for the exergetic evaluation. Third, a levelized cost rate of investment cost and operation-and maintenance (O&M) cost is calculated for each component through an economic analysis. In this paper, we use the total revenue requirement (TRR) method [24] for this analysis. Finally, the exergy and cost values are combined properly by means of the exergy costing principle [10]. By using the results of exergoeconomic calculation, exergoeconomic evaluations are made, which aims at reducing the cost of DX-SAHP from the overall system.

In ref. [16, 25] a detailed procedure for the exergetic, economic, and exergoeconomic analyses were presented. In this paper, we followed the same procedure to analyze experimentally a DX-SAHP system.

2.7 Exergetic Analysis of a Direct Expansion Solar Assisted Heat Pump

Exergetic evaluations are made by using the exergetic variables, such as exergy destruction, exergy destruction ratio, and exergetic efficiency, for each component and for overall system. In exergetic calculation, the exergies of the product and fuel should be defined first, both for each component and for the entire system [4]. The exergy of product ($\dot{E}_{P,k}$) is defined as the desired result of a component (or a system) expressed in exergy value, whereas the exergy of fuel ($\dot{E}_{F,k}$) means the expense of exergy resources to obtain the exergy of product [4]. Table 1 summarizes the definitions of exergy of fuel and product of each component in the DX-SAHP system. The exergy destruction, ($\dot{E}_{D,k}$), the destroyed exergy with in a component during operation, is calculated at the component level as the difference between exergy of fuel and exergy of product, as shown in Eq. (2). The exergetic efficiency is defined as the ratio of the exergy of product and the exergy of fuel; it can be expressed by Eq. (3) for the k-th component, and by Eq. (4) for the overall system. The exergy destruction ratio for each component, y_k, is defined by Eq. (5)

$$\dot{E}_{D,k} = \dot{E}_{F,k} - \dot{E}_{P,k} \quad (2)$$

$$\varepsilon_k = \frac{\dot{E}_{P,k}}{\dot{E}_{F,k}} = \frac{\dot{E}_{F,k} - \dot{E}_{D,k}}{\dot{E}_{F,k}} = 1 - \frac{\dot{E}_{D,k}}{\dot{E}_{F,k}} \quad (3)$$

$$\varepsilon_{tot} = \frac{\dot{E}_{Ptot}}{\dot{E}_{Ftot}} = \frac{\dot{E}_{Ftot} - \dot{E}_{Dtot} - \dot{E}_{Ltot}}{\dot{E}_{Ftot}} = 1 - \frac{\dot{E}_{D,k}}{\dot{E}_{Ftot}} = 1 - \frac{\sum_k \dot{E}_{D,k} - \dot{E}_{Ltot}}{\dot{E}_{Ftot}} \quad (4)$$

$$y_k = 1 - \frac{\dot{E}_{D,k}}{\dot{E}_{Ftot}} \quad (5)$$

Table 1. Definitions of exergy of fuel and exergy of product of each component [21]

Component DX-SAHP	Análisis exergético
Compressor (comp)	$E_{F,comp} = W_{Comp}$ $E_{p,comp} = E_2 - E_1$
Condenser (cond)	$E_{F,cond} = E_2$ $E_{p,cond} = E_3$
Electronic expansion valve (eev)	$E_{F,eev} = E_3$ $E_{p,eev} = E_4$
Solar collector (cs)	$E_{F,cs} = E_7$ $E_{p,cs} = E_8$

The exergy destruction, ($\dot{E}_{D,k}$), the destroyed exergy in the compressor Eq. (6); condenser Eq. (7); electronic expansion valve Eq. (8) and the solar collector Eq. (9) are calculated by [21]

$$\dot{E}_{D,comp} = \dot{E}_{F,k} - \dot{E}_{P,k} + \dot{W}_c \quad (6)$$

$$\dot{E}_{D,cond} = \left(\dot{E}_{F,cond} - \dot{E}_{P,cond}\right) + \left(\dot{E}_{F,ta} - \dot{E}_{P,ta}\right) \quad (7)$$

$$\dot{E}_{D,eev} = \dot{E}_{F,eev} - \dot{E}_{Peev} \quad (8)$$

$$\dot{E}_{D,cs} = \dot{E}_{coll} - \dot{E}_u \quad (9)$$

The useful exergy delivered is calculated by Eq. (10) where $\dot{m}_r$ is the mass flow rate, h_1 is the enthalpy entering to the solar collector, h_2 es the enthalpy leaving the solar collector, T_0 es la Temperature at dead state, and T_e the temperature of evaporation.

$$\dot{E}_{utilizada} = \left[\dot{m}_r(h_1 - h_4)\frac{T_0 - T_e}{T_e}\right] \quad \textbf{(10)}$$

The exergy absorbed by the solar collector is calculated by Eq. (11), where A_c is the area of the solar collector, I, is the average solar irradiation in the solar collector and T_s is the temperature of the solar irradiation where the value of 6000 K is assumed

$$\dot{E}_{colectada} = A_c \dot{I}\left[1 + \frac{1}{3}\left(\frac{T_o}{T_s}\right)^4 - \frac{4}{3}\left(\frac{T_o}{T_s}\right)\right] \quad \textbf{(11)}$$

2.8 Economic Analysis of a Direct Expansion Solar Assisted Heat Pump

As mentioned before, the TRR method was employed to calculate the levelized cost rate of carrying charges ($\dot{Z}^{CC}_k$) and O&M cost ($\dot{Z}^{O\&M}_k$) for each component; the cost rates are used as inputs for the exergoeconomic analysis. In the TRR method, the calculations are conducted through the following steps [16]. First, the purchased equipment cost (PEC_k) data for each component is estimated. Second, the total capital investment (TCI), required for total plant construction, is estimated by using the PEC values and appropriate assumptions. Third, by considering the detailed economic parameters, such as inflation rate, escalation rate, plant life time, depreciation method, interest rates, tax rates, the year-by-year revenue requirement is calculated covering the whole life time of the plant. Finally, the levelized value of revenue requirement is calculated, which leads to the levelized cost of the heat generated [4].

Table 2 shows the cost equations for each component of the DX-SAHP system. To estimate the cost value in dollar ($) of each component ($PEC_k$) is calculated by eq. 12, where the (PEC_{comp}) is the cost of the compressor, (PEC_{cs}) is the cost of the solar collector, (PEC_{evv}) is the cost of a electronic expansion valve and (PEC_{cond}) is the cost of the condenser,

$$\sum PEC_k = PEC_{comp} + PEC_{cs} + PEC_{eev} + PEC_{cond} \quad \textbf{(12)}$$

The total capital investment (TCI), required for total plant construction, is estimated by eq 13 and the total capital investment (TCI), required for total plant construction, is estimated by eq. 14 using the fixed investment capital

$$PEC_{tot} = \sum PEC_k \quad \textbf{(13)}$$

TCI = FCI = Costos directos + Costos indirectos **(14)**

The breakdown of the total capital investment [xx], adapted for a DX-SAHP is shown in table 3

Table 2 Balance equations for the exergoeconomic analysis of a DX-SAHP system

Component DX-SAHP	Análisis exergoeconómico
Compressor (comp)	$c_w\dot{W}_{comp}+\dot{Z}_{comp}=c_2\dot{E}_2-c_1\dot{E}_1$ c_w=0,0000311603 $/KJ
Condenser (cond)	$c_2\dot{E}_2+\dot{Z}_{cond}=c_3\dot{E}_3$
Electronic expansion valve (eev)	$c_3\dot{E}_3+\dot{Z}_{eev}=c_4\dot{E}_4$
Solar collector (cs)	$c_7\dot{E}_7+\dot{Z}_{cs}=c_8\dot{E}_8$ $c_7=0$; $c_8=c_1$

Table 3. Desglose del capital fijo de inversión para bomba de calor de expansión directa asistida por energía solar

1 Costos Directos (DC)		
1.1 Costo de compra de los equipos	15% - 40% de FCI	100% PECk
1.2 Costo de instalación de los equipos	6% -14 % de FCI	20% PECk
1.3 Costo de la estructura metálica	3% -20 % de FCI	7% PECk
1.4 Costo de instrumentración y control	2% - 8% de FCI	40% PECk
1.5 Costo de equipos/materiales eléctricos	2% -10 % de FCI	4% PECk
2 Costos Indirectos (IC)		
2.1 Costo de Ingeniería y supervisión	4% - 21% de FCI	25% PECk
2.2 Costo de construcción	6% - 20% de FCI	15% DC
2.3 Contingencias	5% - 20% de FCI	10% de los costos

To calculate the TRR, assumptions should be made for the economic, financial, operating, and market condition of the country, where the plant should operate. The economic assumptions and parameters, used in this paper, which refer currently to Ecuador, are: The economic lifetime for all components and for the overall system are assumed to be 10 years. The nominal escalation rate of fuel, and the average interest rate are assumed to be 5%, and 12.0%, respectively. The unit cost of electricity is assumed to be $0,00003116/kJ-LCE and corresponds to a levelized cost of the electricity in the year 2019 in Ecuador. As an annual fixed O&M cost, 2 % of the total capital investment (TCI) is allocated to each year [18].

The total required annual revenue in the jth year of operation is obtained from summing the reimbursement cost, electricity cost, and maintenance cost in the jth year and is calculated by eq. (15).

$$TRR_{Jth} = CC_{Jth} + FC_{Jth,electricidad} + OMC_{Jth} \quad \textbf{(15)}$$

The total annual cost over the years is increasing with years of system operation. Therefore, there is a need for levelizing these costs. A capital-recovery factor (CRF) for equivalent amounts in an investment is defined by eq. (16). The total levelized required annual revenue (cost) is calculated by eq. (17).

$$CRF = \frac{i(1+i)^n}{(1+i)^n - 1} \quad \textbf{(16)}$$

$$TRR_L = CRF \sum_{1}^{n} TRR_{Jth} \quad \textbf{(17)}$$

Finally, the levelized annual carrying charge (CC_L), the levelized operation and maintenance cost (OMC_L) is calculated from the eq. (18)

$$CC_L = TRR_L + FC_L - OMC_L \quad \textbf{(18)}$$

The calculated levelized value of carrying charges (CC_L) and (OMC_L) costs are allocated to each component, as shown in Eq. (19), in proportion to their purchased equipment cost. In Eq. (19), the average capacity factor (τ) should be considered to calculate the carrying charges (CC_L) and (OMC_L). The cost of exergy destruction only takes place during the plant operation and is calculated according to Eq. (20).

$$\dot{Z}_k = \dot{Z}_k^{CC} + \dot{Z}_k^{O\&M} = (CC_L + OMC_L)\frac{PEC_k}{\sum PEC_k} x \frac{1}{\tau} \quad \textbf{(19)}$$

$$\dot{C}_{D,k} = c_{F,k}\dot{E}_{D,k} \quad \textbf{(20)}$$

2.9 Exergoeconomic Analysis of a Direct Expansion Solar Assisted Heat Pump

Table 3 summarizes the balance equations and the auxiliary equations, used in the exergoeconomic analysis of the DX-SAHP (The stream numbers are consistent with the numbers used in Fig.1). The cost rate of each exergy stream ($\dot{C}_j$) is calculated by multiplying the specific cost (c_j) and the exergy rate ($\dot{E}_j$) as shown in equation (21); such allocation is called as exergy-costing.

$$\dot{C}_j = c_j \dot{E}_j \quad \textbf{(21)}$$

To obtain all the cj values, the cost balance of each component, shown in Eq. (22), should be formulated based on the exergies of fuel and product concept. Eq. (22) states that the cost of exergy fuel ($\dot{C}_{F,k}$) and the capital investment for carrying charges and O&M costs ($\dot{Z}_k = \dot{Z}^{CC}_k + \dot{Z}^{O\&M}_k$) of k-th component are charged to the cost of exergy of product ($\dot{C}_{p,k}$) of the same component.

$$\dot{C}_{F,k} + \dot{Z}_k = \dot{C}_{P,k} \quad \textbf{(22)}$$

To obtain the specific cost (cj) of each exergy stream, all the balance equations and the auxiliary equations should be solved simultaneously. Auxiliary conditions are required if the component being considered has more

than one outgoing stream; in this paper, the SPECO method [10] is employed to build-up the auxiliary equations: the so-called F-rule and P-rule are used for the exergy fuel side and exergy-product side, respectively. In addition to the equations, derived from the SPECO method, appropriate boundary conditions should be assumed, specifying the overall system's incoming streams.

The exergoeconomic variables, such as the exergoeconomic factor and the relative cost difference [4], can be calculated. Using the exergoeconomic factor shown in Eq. (23), the contribution of capital investment to the overall cost is analyzed. Another important exergoeconomic variable is the relative cost difference (rk), which is defined by Eq. (32). By using the relative cost difference, the components with the highest relative increase between $c_{F,k}$ and $c_{P,k}$ can be identified [40].

$$f_k = \frac{\dot{Z}_k}{\dot{Z}_k + \dot{C}_{D,k}} \tag{23}$$

$$r_k = \frac{c_{P,k} - c_{F,k}}{c_{F,k}} = \frac{\dot{Z}_k + \dot{C}_{D,k}}{c_{F,k}\dot{E}_{P,k}} \tag{24}$$

The $c_{F,k}$ and $c_{P,k}$ used in Eq. (24), are the specific cost of the exergy of fuel and product for the k-th component, respectively, which are calculated using Eqs. (25) and (26).

$$c_{Fk} = \frac{\dot{C}_{F,k}}{\dot{E}_{F,k}} \tag{25}$$

$$c_{Pk} = \frac{\dot{C}_{P,k}}{\dot{E}_{P,k}} \tag{26}$$

3. RESULTS AND DISCUSSION

In this section, the effects on changes in the collector area, rotational compressor displacement (rpm) and the thermoeconomic variables of a DX-SAHP such as exergy destruction, exergy efficiency, the cost rate of exergy destruction rate, total cost rate and exergoeconomic factor for each component are discussed. The exergoeconomic analysis of a DX-SAHP is performed according the model described by [4]. The DX-SAHP thermodynamic cycle is performed according the following parameters: condensing temperature 40-50 °C (variable), collector area 0,75-3m^2 (variable), collector slope 12°, collector efficiency factor 0,85, transmittance-absorptance product 0,9, collector heat loss coefficient 25 W/°C m, compressor efficiency 0,81, compressor displacement 0,00223-0,00378 m^3/s (variable), number of person in house 4, ground reflectance 0,2, average hot water consumption per person 0,07571 m^3/dia. The data of mass flow rate, temperature, pressure, exergy, cost rate and cost rate per exergy unit, at each stream are given in Table 4-6. These data are relative for different configurations of DX-SAHP.

Table 4. Exergoeconomic data for a DX-SAHP for different configurations of solar collector area and 1000 rpm

	a) A_{cs}= 0,75 m^2						b) A_{cs}= 1,5 m^2						c) A_{cs}= 3 m^2					
stream	**ṁ [Kg/s]**	**T [°K]**	**P [Mpa]**	**Ė [kW]**	**c_j ($/kJ)**	**$\dot{C}_j$ ($/h)**	**ṁ [Kg/s]**	**T [°K]**	**P [Mpa]**	**Ė [kW]**	**c_j ($/kJ)**	**$\dot{C}_j$ ($/h)**	**ṁ [Kg/s]**	**T [°K]**	**P [Mpa]**	**Ė [kW]**	**c_j ($/kJ)**	**$\dot{C}_j$ ($/h)**
1	0,027	274,7	0,2519	0,167	3,3E-05	0,01953	0,027	274,45	0,2506	0,6075	1,75E-05	0,0382	0,033	281,85	0,3097	0,341	6,2E-05	0,0764
2	0,027	332,8	1,274	1,108	4,9E-05	0,19531	0,027	334,37	1,3232	1,5686	0,0000	0,21621	0,033	346,01	1,7023	1,5456	5,2E-05	0,2906
3	0,027	312,6	1,0028	0,788	7,7E-05	0,21843	0,027	314,62	1,0572	1,2334	0,0001	0,23881	0,033	322,83	1,3071	0,9882	8,8E-05	0,3132
4	0,027	296,5	0,6333	0,763	9,7E-05	0,2671	0,027	289,18	0,5048	1,1777	0,0001	0,28641	0,033	292,31	0,5567	0,8928	0,00011	0,3607

Table 5. Exergoeconomic data for a DX-SAHP for different configurations of solar collector area and 1350 rpm

	a) A_{cs}= 0,75 m^2						b) A_{cs}= 1,5 m^2						c) A_{cs}= 3 m^2					
stream	**ṁ [Kg/s]**	**T [°K]**	**P [Mpa]**	**Ė [kW]**	**c_j ($/kJ)**	**$\dot{C}_j$ ($/h)**	**ṁ [Kg/s]**	**T [°K]**	**P [Mpa]**	**Ė [kW]**	**c_j ($/kJ)**	**$\dot{C}_j$ ($/h)**	**ṁ [Kg/s]**	**T [°K]**	**P [Mpa]**	**Ė [kW]**	**c_j ($/kJ)**	**$\dot{C}_j$ ($/h)**
1	0,031	270,2	0,2116	0,587	9,7E-06	0,0205	0,033	272,15	0,2294	0,69	1,6E-05	0,0403	0,035	273,25	0,2408	0,7607	2,8E-05	0,078
2	0,031	334,9	1,3103	1,798	3,7E-05	0,23807	0,033	337,3	1,4025	1,99	3,8E-05	0,2704	0,035	340	1,5058	2,1375	4,1E-05	0,3184
3	0,031	314,5	1,0551	1,416	5,1E-05	0,26227	0,033	316,56	1,1129	1,54	5,3E-05	0,2943	0,035	318,89	1,1822	1,6188	5,9E-05	0,3415
4	0,031	296,7	0,637	1,381	6,3E-05	0,31327	0,033	289,84	0,5155	1,46	6,6E-05	0,3446	0,035	286,58	0,4642	1,5061	7,2E-05	0,3901

Table 6. Exergoeconomic data for a DX-SAHP for different configurations of solar collector area and 1700 rpm

	a) A_{cs}= 0,75 m^2						b) A_{cs}= 1,5 m^2						c) A_{cs}= 3 m^2					
stream	**ṁ [Kg/s]**	**T [°K]**	**P [Mpa]**	**Ė [kW]**	**c_j ($/kJ)**	**$\dot{C}_j$ ($/h)**	**ṁ [Kg/s]**	**T [°K]**	**P [Mpa]**	**Ė [kW]**	**c_j ($/kJ)**	**$\dot{C}_j$ ($/h)**	**ṁ [Kg/s]**	**T [°K]**	**P [Mpa]**	**Ė [kW]**	**c_j ($/kJ)**	**$\dot{C}_j$ ($/h)**
1	0,037587	269,1	0,2037	0,607	1,7E-05	0,0382	0,038146	269,95	0,2077	0,7086	1,66E-05	0,0423	0,04128	273,95	0,2278	0,1584	0,00014	0,0826
2	0,037587	337,5	1,3926	1,569	3,8E-05	0,21621	0,038146	340,26	1,4735	2,3199	3,84E-05	0,32058	0,04128	348,75	1,7426	1,985	5,7E-05	0,405
3	0,037587	325	1,379	1,233	5,4E-05	0,23881	0,038146	318,5	1,1706	1,7643	5,44E-05	0,34558	0,04128	323,7	1,3361	1,2533	9,5E-05	0,4294
4	0,037587	300,6	0,714	1,178	6,8E-05	0,28641	0,038146	290,91	0,5331	1,672	6,62E-05	0,39828	0,04128	290,48	0,5259	1,1124	0,00012	0,4676

Thermoeconomic variables of DX-SAHP, exergy destruction, exergy efficiency, average unit cost of fuel and product, the cost rate of exergy destruction rate, total cost rate and exergoeconomic factor for each component are given in Table 7-9

Table 7. The thermoeconomic variables for a DX-SAHP for different configurations of solar collector area and 1000 rpm

DX-SAHP Configurations	Theromoeconomics variables	Components			
		Compressor	Condenser	Electronic expansion valve	Solar Collector
0,75 m^2	ED [kW]	0,30	0,32	0,03	0,32
1000 rpm	Ɛ [%]	76%	71%	97%	16%
	cF [$/kJ]	3,12E-05	4,90E-05	7,70E-05	1,96E-04
	cP [$/kJ]	5,19E-05	7,70E-05	9,72E-05	1,30E-03
	ĊD [$/h]	0,034103	0,056263	0,007077	0,223706
	Żk [$/h]	0,0362	0,0231	0,0487	0,0195
	rk [%)	66%	57%	26%	561%
	f [%]	51%	29%	87%	8%
1,5 m^2	ED [kW]	0,31	0,34	0,06	0,64
1000 rpm	Ɛ [%]	76%	79%	95%	20%
	cF [$/kJ]	3,12E-05	3,83E-05	5,38E-05	9,97E-05
	cP [$/kJ]	5,14E-05	5,38E-05	6,76E-05	5,69E-04
	ĊD [$/h]	0,034842	0,046210	0,010773	0,229525
	Żk [$/h]	0,0354	0,0226	0,0476	0,0382
	rk [%)	65%	40%	26%	471%
	f [%]	50%	33%	82%	14%
3 m^2	ED [kW]	0,39	0,56	0,10	2,92
1000 rpm	Ɛ [%]	76%	64%	90%	4%
	cF [$/kJ]	3,12E-05	5,22E-05	8,80E-05	3,28E-05
	cP [$/kJ]	4,94E-05	8,80E-05	1,12E-04	9,12E-04
	ĊD [$/h]	0,043666	0,104780	0,030243	0,345000
	Żk [$/h]	0,0354	0,0226	0,0476	0,0764
	rk [%)	58%	69%	28%	2677%
	f [%]	45%	18%	61%	18%

Table 8. The thermoeconomic variables for a DX-SAHP for different configurations of solar collector area and 1350 rpm

DX-SAHP Configurations	Theromoeconomics variables	Components			
		Compressor	Condenser	Electronic expansion valve	Solar Collector
0,75 m^2	ED [kW]	0,39	0,38	0,03	0,30
1350 rpm	Ɛ [%]	76%	79%	98%	18%
	cF [$/kJ]	3,12E-05	3,68E-05	5,15E-05	2,39E-04
	cP [$/kJ]	4,99E-05	5,15E-05	6,30E-05	1,43E-03
	ĊD [$/h]	0,043896	0,050564	0,006407	0,257467
	Żk [$/h]	0,0379	0,0242	0,0510	0,0205
	rk (%)	60%	40%	22%	498%
	f [%]	46%	32%	89%	7%
1,5 m^2	ED [kW]	0,42	0,45	0,08	0,59
1350 rpm	Ɛ [%]	76%	77%	95%	23%
	cF [$/kJ]	3,12E-05	3,77E-05	5,32E-05	1,24E-04
	cP [$/kJ]	4,92E-05	5,32E-05	6,55E-05	5,95E-04
	ĊD [$/h]	0,047067	0,061629	0,014492	0,264140
	Żk [$/h]	0,0374	0,0239	0,0503	0,0403
	rk (%)	58%	41%	23%	379%
	f [%]	44%	28%	78%	13%
3 m^2	ED [kW]	0,44	0,52	0,11	0,68
1350 rpm	Ɛ [%]	76%	76%	93%	26%
	cF [$/kJ]	3,12E-05	4,14E-05	5,86E-05	1,17E-04
	cP [$/kJ]	4,85E-05	5,86E-05	7,19E-05	5,41E-04
	ĊD [$/h]	0,049910	0,077256	0,023771	0,288648
	Żk [$/h]	0,0361	0,0231	0,0486	0,0780
	rk (%)	55%	42%	23%	361%
	f [%]	42%	23%	67%	21%

Table 9. The thermoeconomic variables for a DX-SAHP for different configurations of solar collector area and 1700 rpm

DX-SAHP Configurations	Theromoeconomics variables	Components			
		Compressor	Condenser	Electronic expansion valve	Solar Collector
0,75 m^2	ED [kW]	0,50	0,47	0,07	0,75
1700 rpm	Ɛ [%]	76%	71%	94%	1%
	cF [$/kJ]	3,12E-05	5,02E-05	7,70E-05	1,36E-04
	cP [$/kJ]	4,84E-05	7,70E-05	9,64E-05	1,18E-02
	ĊD [$/h]	0,056343	0,085015	0,020688	0,368005
	Żk [$/h]	0,0403	0,0257	0,0542	0,0217
	rk (%)	55%	53%	25%	8635%
	f [%]	42%	23%	72%	6%
1,5 m^2	ED [kW]	0,52	0,56	0,09	1,36
1700 rpm	Ɛ [%]	76%	76%	95%	12%
	cF [$/kJ]	3,12E-05	3,84E-05	5,44E-05	7,19E-05
	cP [$/kJ]	4,80E-05	5,44E-05	6,62E-05	6,81E-04
	ĊD [$/h]	0,058411	0,076784	0,018069	0,351816
	Żk [$/h]	0,0392	0,0250	0,0527	0,0423
	rk (%)	54%	42%	22%	848%
	f [%]	40%	25%	74%	11%
3 m^2	ED [kW]	0,59	0,73	0,14	2,88
1700 rpm	Ɛ [%]	76%	63%	89%	6%
	cF [$/kJ]	3,12E-05	5,67E-05	9,52E-05	4,22E-05
	cP [$/kJ]	4,90E-05	9,52E-05	1,17E-04	7,83E-04
	ĊD [$/h]	0,066214	0,149290	0,048298	0,437982
	Żk [$/h]	0,0514	0,0244	0,0382	0,0826
	rk (%)	57%	68%	23%	1756%
	f [%]	44%	14%	44%	16%

3.1 Result of The Exergetic Analysis

Figure 3 shows the variation of exergy destruction with three solar collector area and three different rotational compressor displacements. In this figure one observes that the solar collector is the most exergy destructive component of the DX-SAHP, reaching their highest point at 1700 rpm for all three configurations of solar collector. This is due that the increase of rotational velocity of the compressor producing a greater flux mass of the refrigerant and therefore a greater friction of refrigerant fluid. Friction and heat transfer loss are two factors that contribute to exergy destruction. The least exergy destructive component of the DX-SAHP is the electronic expansion valve

within a range of 0,03 y 0,14 kW. The compressor is found to be in the range of 0,32 y 0,62 kW and the condenser among 0,03 y 0,14 kW

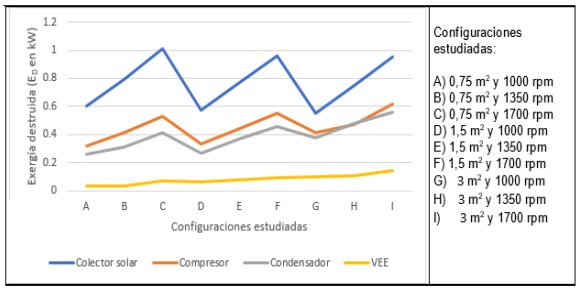

Fig 3. Variation of exergy destruction for different configurations of solar collector and rotational compressor displacement

Figure 4 shows the variation of exergy efficiency with three solar collector area and three different rotational compressor displacements. The solar collector exergetic efficiency is in the range of 3 to 26% this is the lowest value among the DX-SAHP components which is due to low exergy at collector product compared with collector fuel. The electronic expansion valve is the most exergetic efficiency component between a range of 89 and 98%. The compressor and the condenser show values relatively higher.

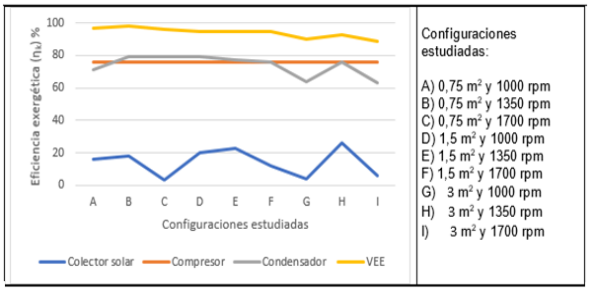

Fig. 4. Variation of exergy efficiency for different configurations of solar collector and rotational compressor displacement

3.2 Result of the Exergoeconomic Analysis

The result obtained from the exergy destruction cost for different configurations of solar collector and rotational compressor displacement is shown in Fig. 5. The exergy destruction cost was highest for the solar collector reaching their highest point (0,44 $/h) for 3 m^2 area of solar collector at 1700 rpm and lowest for the electronic expansion valve within a range of 0,007 a 0,048 $/h.

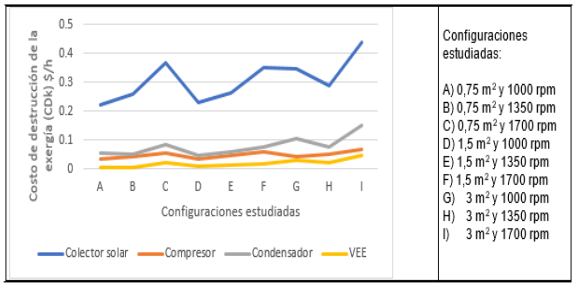

Fig. 5: Variation of exergy destruction cost for different configurations of solar collector and rotational compressor displacement

Figure 6 shows the total exergy cost for each one of the components of a DX-SAHP with three solar collector area and three different rotational compressor displacements. The total exergy cost was highest for the solar collector compressor within a range of 0,24 and 0,52 $/h, and was lowest for the electronic expansion valve within a range of 0,07 y 0,17 $/h for all the configurations studied. The total exergy cost of the electronic expansion valve was lowest due to the lower exergy destruction as compared to the solar collector even though it has a high purchasing cost of the expansion device.

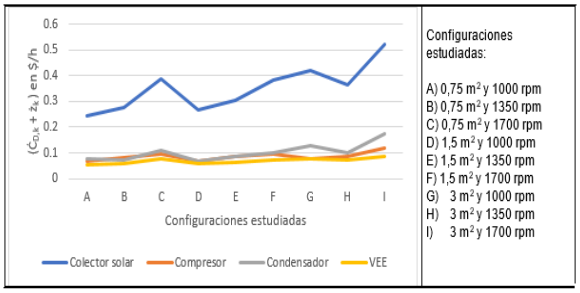

Fig. 6. Total exergy cost for different configurations of solar collector and rotational compressor displacement

The electronic expansion valve was having the highest values of the exergoeconomic factor within the range of 44 to 89% followed by the compressor between 41 to 51 %. The exergoeconomic factor values were lowest for the solar collector among 5 to 21% as shown in Fig. 7

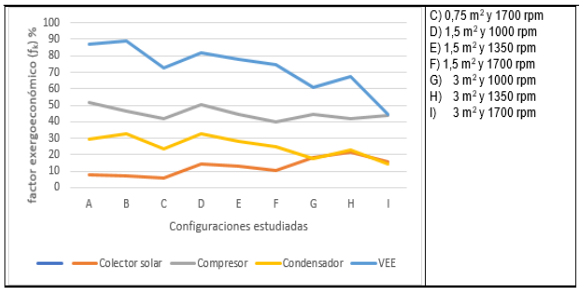

Fig. 7: Exergoeconomic factor for different configurations of solar collector and rotational compressor displacements.

When evaluating the components of direct expansion solar assisted heat pump through their exergoeconomic factor, the following suggestions are taken into account to reduce the final cost of the system: The electronic expansion valve that exhibits a high exergoeconomic factor is suggested to be lowered. the cost of this, for example, by acquiring a cheaper technology, even if this implies an increase in the costs of exergy and the destruction of exergy. For the solar collector and the compressor that show relatively low values of exergoeconomic factor, it is necessary to improve the thermodynamic efficiency, although this improvement in thermodynamic efficiency implies an increase in the capital investment costs of these components, for the components that show a value intermediate exergoeconomic factor such as the compressor,

CONCLUSIONS

A direct expansion solar assisted heat pump was evaluated from an exergoeconomic point of view, the analysis presented in this study demonstrate the effect of the solar collector in the optimization of the energetic system. The exergoeconomic data at each stream of a DX-SAHP are shown at tables 4-6 respectively.

The exergoeconomic variables at each component of DX-SAHP for different configurations of solar collector area and rotational velocity of the compressor are shown at Figures 3-7. Data of exergy destruction, exergy

efficiency, the cost rate of exergy destruction rate, total cost rate, and exergoeconomic factor or each component are discussed.

Through the exergoeconomic analysis, the cost structure of the DX-SAHP is analyzed and the exergoeconomic factor of each component is obtained. The highest exergoeconomic factor, is observed on the electronic expansion valve and the lowest value, is calculated for the solar collector. Depending on the value of exergoeconomic factors, different strategies are suggested for individual components, targeting the cost reduction of the final product from the overall system.

ACKNOWLEGDMENTS

The authors appreciate the support of The Technical University of Manabí (UTM) and the Technical University of Havana “José Antonio Echeverria” for the support given for the present research.

REFERENCES

[1] Kong, X., et al., Influence of different regulation modes of compressor speed on the performance of direct-expansion solar-assisted heat pump water heater. Applied Thermal Engineering, 2020. 169: p. 115007.

[2] Huang, W., et al., Numerical study and experimental validation of a direct-expansion solar-assisted heat pump for space heating under frosting conditions. Energy and Buildings, 2019. 185: p. 224-238.

[3] Şevik, S., et al., Mushroom drying with solar assisted heat pump system. Energy Conversion and Management, 2013. 72: p. 171-178.

[4] Bejam, A., G. Tsatsaronis, and M. Moran, Thermal Design and Optimization, ed. I. Jhon Wiley & Sons. 1996, Canada. 542.

[5] Badiei, A., et al., A chronological review of advances in solar assisted heat pump technology in 21st century. Renewable and Sustainable Energy Reviews, 2020. 132: p. 110132.

[6] Shi, G.-H., et al., Recent advances in direct expansion solar assisted heat pump systems: A review. Renewable and Sustainable Energy Reviews, 2019. 109: p. 349-366.

[7] Tsatsaronis, G., T. Morosuk, and M. Schult, Conventional and Advanced Exergetic Analyses: Theory and Application. Arabian Journal for Science and engineering, 2013. 38(2): p. 395-404.

[8] Tsatsaronis, G. and T. Morosuk, Understanding and improving energy conversion systems with the aid of exergy-based methods. Int. J. Exergy, 2012. 11(4): p. 518-42.

[9] Tatiana, M., T. George, and S. Marco., Conventional and Advanced Exergetic Analyses: Theory and Application. Arabian Journal for Science and Engineering, 2013. 38(2): p. 395-404.

[10] Lazzaretto, A. and G. Tsatsaronis, SPECO: A systematic and general methodology for calculating efficiencies and costs in thermal systems. Energy, 2006. 31(8–9): p. 1257-1289.

[11] Yew, L. K. ., Kowang, T. O. ., Yang, M. ., & Jong, L. C. . (2023). Consumers Purchase Intention towards Solar Panel as Renewable Energy Source in Malaysia. International Journal of Membrane Science and Technology, 10(3), 1786-1796. https://doi.org/10.15379/ijmst.v10i3.1805

[12] Chaturvedi, S.K., V.D. Gagrani, and T.M. Abdel-Salam, Solar-assisted heat pump – A sustainable system for low-temperature water heating applications. Energy Conversion and Management, 2014. 77: p. 550-557.

[13] Rabelo, S.N., et al., Economic analysis and design optimization of a direct expansion solar assisted heat pump. Solar Energy, 2019. 188: p. 164-174.

[14] Hepbasli, A., H. Ozcan, and H. Gunerhan, Thermoeconomic Analysis of a Mobile Air Conditioning Unit Using the Specific Exergy Cost (SPECO) Method IOP Conference Series: Earth and Environmental Science, 2020. 464 012010.

[15] Singh, A., J. Sarkar, and R.R. Sahoo, Experimental energy, exergy, economic and exergoeconomic analyses of batch-type solar-assisted heat pump dryer. Renewable Energy, 2020.

[16] Abusoglu, A. and M. Kanoglu, Exergoeconomic analysis and optimization of combined heat and power production: A review. Renewable and Sustainable Energy Reviews, 2009. 13(9): p. 2295-2308.

[17] Lee, Y.D., et al., Exergetic and exergoeconomic evaluation of an SOFC-Engine hybrid power generation system. Energy, 2018. 145: p. 810-822.

[18] HAMID, M., Jam, F.A., Mehmood, S. (2019). Psychological Empowerment and Employee Attitudes: Mediating Role of Intrinsic Motivation. International Journal of Business and Economic Affairs, 4(6), 300-314.

[19] Cavalcanti, E., Exergoeconomic and exergoenvironmental analyses of an integrated solar combined cycle system. Renewable and Sustainable Energy Reviews 2017. 67(2017): p. 507-519.

[20] Shams Ghoreishi, S.M., et al., Analysis, economical and technical enhancement of an organic Rankine cycle recovering waste heat from an exhaust gas stream. Energy Science & Engineering, 2019.

[21] Holman, J.P., Experimental methods for engineers 8th ed ed. 2012.

[22] Gorozabel Chata, F.B. and T. Carbonell Morales, Análisis energético y exergético de una bomba de calor de expansión directa con energía solar. Ingeniería Energética, 2020. 41(e1210): p. 1-11.

[23] Kara, O., K. Ulgen, and A. Hepbasli, Exergetic assessment of direct-expansion solar-assisted heat pump systems: Review and modeling. Renewable and Sustainable Energy Reviews, 2008. 12(5): p. 1383-1401.

[24] Mohanraj, M., S. Jayaraj, and C. Muraleedharan, Exergy analysis of direct expansion solar-assisted heat pumps using artificial neural networks. International Journal of Energy Research, 2009. 33(11): p. 1005-1020.

[25] Mohanraj, M., S. Jayaraj, and C. Muraleedharan, Exergy Assessment of a Direct Expansion Solar-Assisted Heat Pump Working with R22 and R407C/LPG Mixture. International Journal of Green Energy, 2010. 7(1): p. 65-83.

[26] NREL. National Renewable Energy Laboratory, A Manual for the Economic Evaluation of Energy Efficiency and Renewable Energy Technologies ed. NREL/TP-462-5173. 1995, Golden Colorado National Renewable Energy Laboratory

[27] Lee, Y.D., et al., Exergetic and exergoeconomic evaluation of a solid-oxide fuel-cell-based combined heat and power generation system. Energy Conversion and Management, 2014. 85: p. 154-164.

DOI: https://doi.org/10.15379/ijmst.v10i4.2110